Asian Journal of Chemistry; Vol. 37, No. 11 (2025), 2712-2724
ASIAN JOURNAL OF CHEMISTRY
https://doi.org/10.14233/ajchem.2025.34581

Novel 1,3,4-Oxadiazolyltriazole-Derived Phthalazine Scaffolds: Design, Synthesis, Bioactive Evaluation and Computational Docking Study

PULLARAO PERLA[1,2], THIYYAKUR YAMINI[1], DEEPTI KOLLI[1,*], MOHAMED TAKHI[2], SRINU BHOOMANDLA[3] and PILLI V.V.N. KISHORE[4]

[1]Department of Chemistry, Koneru Lakshmaiah Education Foundation, Green Fields, Vaddeswaram, Guntur-522302, India
[2]United States Pharmacopeia India (P) Ltd., Plot No. D6 & D8, IKP, Genome Valley, Shamirpet, Hyderabad-500101, India
[3]Department of Chemistry, School of Science, GITAM (Deemed to be University), Hyderabad-502329, India
[4]Department of Chemistry, School of Applied Sciences and Humanities, Vignan's Foundation for Science Technology and Research, Vadlamudi, Guntur-522213, India

*Corresponding author: E-mail: atluri.deepti1984@gmail.com

Received: 31 July 2025 *Accepted*: 13 September 2025 *Published online*: 27 October 2025 AJC-22158

In this study, a series of novel hybrid compounds comprising phthalazine and 1,3,4-oxadiazolyl–triazole moieties were synthesized. The structures of all synthesized compounds were characterized using FT-IR, ^{1}H NMR, ^{13}C NMR and mass spectrometric techniques. The antibacterial and antifungal activity of synthesized compounds was assessed *in vitro* using the inhibitory zone method against strains of fungi, Gram-negative and Gram-positive bacteria with the largest inhibition zone diameters ranging from 35.80 to 45.01 mm, respectively. Among the tested compounds, **5a**, **5e**, **7a** and **7d** demonstrated the superior antibacterial activity against *S. aureus* and *E. coli* when compared to the standard medication (levofloxacin). Compound **7d** showed potent antifungal activity with zone of inhibition values of 30.24 ± 0.14 and 31.56 ± 1.20 mm against *A. flavus* and *C. albicans*, respectively. Furthermore, the most bacterial strains rely on DNA gyrase for nucleic acid synthesis, molecular docking studies were conducted against DNA gyrase from *S. aureus* (PDB ID: 2XCR) and topoisomerase IV from *E. coli* (PDB ID: 1S14). These results suggest that compound **7d** holds a potential lead compound for the development of new antibiotics. The molecular docking analysis of compounds **5a**, **7a** and **7d** demonstrated a good interaction with the target protein with a high docking score of -7.52, -7.12 and -6.96 kcal/mol, respectively. The synthesized novel compounds represent a valuable scaffold that can be further optimized to develop potent antimicrobial agents for future therapeutic applications.

Keywords: 1,2,3-Triazole, 1,3,4-Oxadiazole, Phthalazine, Antimicrobial activity, *In silico* docking, ADMETlab3.0.

INTRODUCTION

Microbial diseases and its controls are a growing global threat to both public health and the economy [1]. The effectiveness of traditional antibiotics in treating bacterial infections has significantly declined [2]. In recent years, humanity has faced serious challenges from microbial diseases such as plague, cholera, diphtheria, typhoid fever, tuberculosis and various respiratory infections [3]. The most prevalent bacterial infections that result in death in most affluent nations are caused by *Staphylococcus epidermidis*, vancomycin-resistant *Enterococci* and methicillin-resistant *Staphylococcus aureus* (MRSA) [4,5]. The WHO states that conventional antibiotic therapy is often ineffective against antibiotic-resistant bacteria. This significantly increases the risk of treatment failure, prolongs illness and suffering, raises the likelihood of complications and ultimately contributes to higher mortality rates [6]. As a result, it is still required to produce innovative antimicrobial medications that are distinct from the popular classes of antibacterial agents [7]. Furthermore, one potential solution to the problem of excessive multidrug resistance (MDR) is the development of novel drugs with distinct mechanisms of action to prevent cross-resistance with already available pharmaceuticals [8]. Heterocyclic ring structures in organic compounds continue to attract a lot of attention due to their wide range of biological functions.

The importance in bioactivity and synthetic potential, triazoles and their related heterocyclic derivatives have garnered a lot of interest recently [9]. Azolic derivatives, such as triazole, thiazole, oxadiazole and thiadiazole, are pharmacologically

This is an open access journal, and articles are distributed under the terms of the Attribution 4.0 International (CC BY 4.0) License. This license lets others distribute, remix, tweak, and build upon your work, even commercially, as long as they credit the author for the original creation. You must give appropriate credit, provide a link to the license, and indicate if changes were made.

active substances in medicinal chemistry [10] and they are used in the treat of leishmaniasis, diabetes, bacteria, viruses, tuberculosis, cancer, malaria and neuroprotection [11]. The 1,2,3-triazole compounds have demonstrated a wide range of pharmacological activities [12-14]. Various biological activities of 1,3,4-oxadiazoles are also well known, including antimicrobial [15], antifungal [16], anti-inflammatory, analgesic [17], anticancer [18], anti-spasmolytic and hypotensive [19], anti-proliferative [20], anticonvulsant [21], anti-allergic and enzymatic inhibitors [22]. The well-known drugs on the market are raltegravir, furamizole, zibotentan, ataluren and nesapidil (Fig. 1) [23,24].

Phthalazines are widely recognized as valuable pharmacophores, serving as the core compound scaffold in several commercially available drugs. Notable examples include vatalanib, an angiogenesis inhibitor; budralazine, a vasodilator; azelastine, an antihistamine; carbazeran, used in the treatment of heart failure and hydralazine, an antihypertensive agent [25,26]. Phthalazine derivatives acts as high-affinity ligands of voltage-gated calcium channels, selective binders of GABA receptors, cyclooxygenase-2 inhibitors and p38MAP kinase inhibitors (Fig. 1) [27-33]. These factors suggest the necessity of continuing attempts to develop selective antibacterial drug-like candidates having minimal side-effects. Therefore, the focus of current research is on synthesized new, safer antimicrobial agents which are essential for usage in the clinical research.

Further the docking interactions of the prepared ligands were performed using the crystal structures of DNA gyrase and topoisomerase-IV inhibitors. Furthermore, the target compounds were exposed to *in silico* molecular properties prediction and drug resemblance by employing online web server called SwissADME, ADMETlab3.0 [34].

EXPERIMENTAL

All chemicals, reagents and solvents used were of commercial grade and procured from Hyma, Merck, Spectrochem, and Sigma-Aldrich. The IKON melting point apparatus was used to measure the uncorrected melting points in open capillaries. Thin layer chromatography (TLC) was used to monitor the reactions (1:9) using Merck silica gel $60F_{254}$ plates and ethyl acetate:hexane. The compounds were visible under a UV lamp A 60-120 mesh silica gel was employed in column chromatography. The Binary Gradient HPLC-3000 equipment was used to verify the purity of synthesized phthalazine products. Using KBr disc, IR spectra were acquired using a Perkin-Elmer spectrophotometer (Spectrum-Two); values are given ν in cm^{-1}. Bruker 400 MHz and 100 MHz were used to record the ^{1}H and ^{13}C NMR spectra, respectively. The compounds mass spectra were obtained using the Advion Expression-S CMS instrument.

Synthesis of 4-ethyl-2-((5-mercapto-1,3,4-oxadiazol-2-yl)methyl)phthalazin-1(2*H*)-one (2): Absolute ethanol (15 mL)

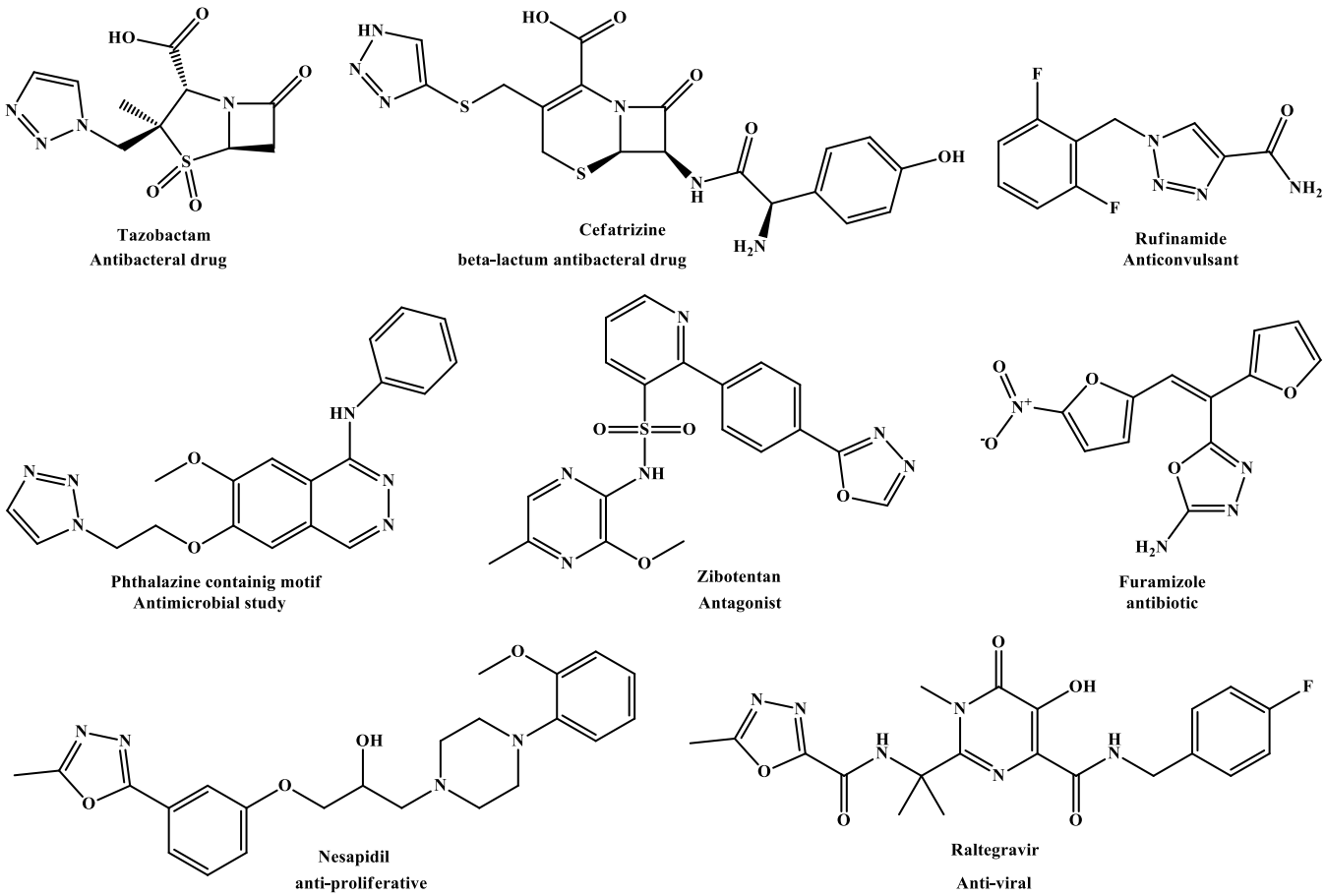

Fig. 1. Structure of some commercially available drugs containing triazole, oxadiazole and phthalazine core

was used to suspend hydrazine product of 2-(4-ethyl-1-oxophthalazin-2(1*H*)-yl)acetohydrazide (**1**, 1.2 g, 4.8 mmol). Carbon disulfide (0.7 g, 9.7 mmol, 1.2 equiv.) and KOH (0.4 g, 7.2 mmol, 1.5 equiv.) were then added at > 10 ºC for 20 min. At 60 ºC, the resultant suspension was agitated for 10 h. The reaction mixture was then extracted using ethyl acetate (2 × 50 mL) after being diluted with 100 mL of water. After being separated, the organic layer was dried over Na_2SO_4 and then evaporated using a rotary evaporator. After being redissolved in DCM, the residue was put through chromatography on silica gel using 5% methanol in methylene chloride as eluent. Pale yellow foam was obtained (yield: 81%; m.p.: 128 ºC).

Synthesis of 4-ethyl-2-((5-(prop-2-yn-1-ylthio)-1,3,4-oxadiazol-2-yl)methyl)phthalazin-1 (2*H*)-one (3): The procedure used for propargylation was reported in literature [35]. A 25 mL of $NaHCO_3$ solution (0.7 g, 9.3 mmol, 1.8 equiv.) and (0.86 g, 7.2 mmol, 1.4 equiv.) of propargyl bromide were added to a solution of oxadiazole compound (**2**, 1.5 g, 5.2 mmol) in DMF (15 mL) in a different round-bottom flask while being vigorously stirred at room temperature. For 7 h, the mixture was left to react at 90 ºC. TLC was used to track the reaction's progress (DCM:MeOH, 9:1). The obtained propargylated product **3** (yield 87%, m.p.: 110 ºC) was purified by column chromatography using a DCM:MeOH (98:2) mixture as eluent after the solvent was evaporated.

General procedure for the synthesis of azides 4a-e: Azides were synthesized using the reported procedure [5]. A solution of (4-nitrophenyl)methanamine (2.5 g, 16.4 mmol) in 20 mL of DCM at 0 ºC was placed in a 250 mL round flask. Small amounts of sodium nitrite (2.2 g, 32.8 mmol, 2 equiv.) were added under nitrogen atmosphere. The reaction mass was agitated for approximately 30 min at 25-30 ºC after the addition was finished. During 30 min at 10-15 ºC in a nitrogen environment, AcOH (1.48 g, 24.6 mmol, 1.5 equiv.) and $N_2H_4 \cdot H_2O$ (4.1 g, 82.2 mmol, 5 equiv.) in 10 mL of DCM were added to the reaction mass. Following addition, the reaction mass was agitated for 2.5 h at 25-30 ºC. The progress of the reaction was tracked by TLC (EtOAc:hexane 1:9). Following the completion of the reaction, 200 mL of distilled water were added and the mixture was acidified with dil. HCl until pH 4. After that, stirring continued for 0.5 h. To obtain 1-(azidomethyl)-4-nitrobenzene (**4a**), the cyclized material was then extracted in ethyl acetate (2 × 75 mL), dried over anhydrous sodium sulfate and evaporated under vacuum. The remaining azide compounds **4b-e** were also synthesized by following the above described method and then utilized in the following step without being purified.

General procedure for the synthesis of 5a-e: The method described in the literature was used to synthesize triazoles [36]. A solution of DMF and water (3:2) was used to suspend compounds **3** (1 equiv.) and substituted aromatic azides (**4a-e**, 1.5 equiv.). After that, a $CuSO_4 \cdot 5H_2O$ solution (0.7 equiv.) and a sodium ascorbate solution (0.9 equiv.) were added. The heterogeneous mixture was quickly agitated at room temperature until the alkyne was consumed and TLC was used to track the development of the reaction. The precipitate, was obtained by pouring the reaction mixture into freezing water once the reaction was finished. A $CHCl_3$:MeOH (97:3) mixture was used as eluent in column chromatography to purify the products (**Scheme-I**).

4-Ethyl-2-((5-(((1-(4-nitrobenzyl)-1*H*-1,2,3-triazol-4-yl)methyl)thio)-1,3,4-oxadiazol-2-yl)methyl)phthalazin-1-(2*H*)-one (5a): Yellow solid; yield: 83%, m.p.: 134-136 ºC. ^{1}H NMR (DMSO-d_6, 500 MHz) δ ppm: 1.64 (t, 3H, *J* = 10.2 Hz, CH_3), 2.23 (q, 2H, *J* = 10.8 Hz, CH_2), 4.29 (s, 2H, NCH_2), 4.74 (s, 2H, SCH_2), 5.42 (s, 2H, NCH_2), 7.27 (d, 2H, *J* = 9.4 Hz, Ar-H), 7.37 (t, 1H, *J* = 10.2 Hz, Ar-H), 7.46 (s, 1H, triazole-H), 7.55 (t, 1H, *J* = 10.2 Hz, Ar-H), 7.90 (d, 1H, *J* = 9.6 Hz, Ar-H), 8.19 (d, 2H, *J* = 9.4 Hz, Ar-H), 8.28 (d, 1H, *J* = 9.6 Hz, Ar-H); ^{13}C NMR (DMSO-d_6, 125 MHz) δ ppm: 14.44 (CH_3), 33.76 (CH_2), 36.47 (SCH_2), 51.49 (NCH_2), 59.14 (NCH_2), 120.89, 126.50, 126.73, 129.06, 130.17, 134.14, 136.66, 138.38, 139.06, 140.49, 144.49, 148.13, 161.42 (oxadiazole-C), 164.02 (CO); IR (KBr, ν_{max}, cm^{-1}): 1193.85 (COC), 1248.00 (CSC), 1345.38 (N-N), 1471.37 (C=N), 1587.38 (C=C), 1638.67 (CO), 2924.76 (CH), 3055.39 (=CH). Mass (*m/z*): 505.32 $[M + H]^+$. Elemental analysis of $C_{23}H_{20}N_8O_4S$: Calcd. (found) %: C, 54.76 (54.54); H, 4.00 (3.89); N, 22.21 (22.09); S, 6.35 (6.24).

4-Ethyl-2-((5-(((1-(4-methoxybenzyl)-1*H*-1,2,3-triazol-4-yl)methyl)thio)-1,3,4-oxadiazol-2-yl)methyl)phthalazine-1(2*H*)-one (5b): Light grey colour solid; yield: 76%, m.p.: 113-115 ºC. ^{1}H NMR (DMSO-d_6, 500 MHz) δ ppm: 1.80 (t, 3H, *J* = 10.2 Hz, CH_3), 2.91 (q, 2H, *J* = 10.8 Hz, CH_2), 3.84 (s, 3H, OCH_3), 4.14 (s, 2H, NCH_2), 4.70 (s, 2H, SCH_2), 5.53

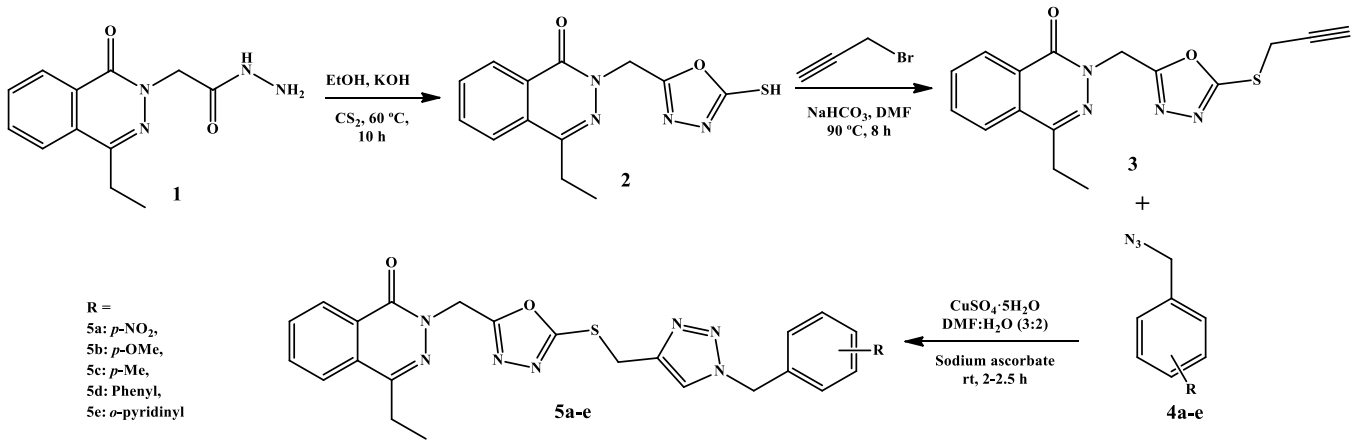

Scheme-I: Synthesis of novel 1,3,4-oxadiazole & 1,2,3-triazole precursors

(s, 2H, NCH_2), 6.89 (d, 2H, *J* = 9.4 Hz, Ar-H), 7.24 (d, 2H, *J* = 9.4 Hz, Ar-H), 7.40 (t, 1H, *J* = 10.2 Hz, Ar-H), 7.57 (s, 1H, triazole-H), 7.61 (t, 1H, *J* = 10.2 Hz, Ar-H), 8.12 (d, 1H, *J* = 9.6 Hz, Ar-H), 8.38 (d, 1H, *J* = 9.6 Hz, Ar-H); ^{13}C NMR (DMSO-d_6, 125 MHz) δ ppm: 14.91 (CH_3), 32.61 (CH_2), 36.35 (SCH_2), 51.24 (NCH_2), 56.32 (OCH_3), 59.77 (NCH_2), 113.68, 120.88, 126.67, 129.54, 129.68, 129.84, 133.78, 137.73, 139.14, 140.48, 147.13, 154.49, 161.42 (oxadiazole-C), 164.01 (CO). IR (KBr, ν_{max}, cm^{-1}): 1185.14 (COC), 1242.08 (CSC), 1341.43 (N-N), 1479.30 (C=N), 1583.87 (C=C), 1639.67 (CO), 2925.67 (CH), 3017.53 (=CH). Mass (*m/z*): 490.30 $[M + H]^+$. Elemental analysis of $C_{24}H_{23}N_7O_3S$: Calcd. (found) %: C, 58.88 (58.71); H, 4.74 (4.62); N, 20.03 (19.89); S, 6.55 (6.34).

4-Ethyl-2-((5-(((1-(4-methylbenzyl)-1*H*-1,2,3-triazol-4-yl)methyl)thio)-1,3,4-oxadiazol-2-yl)methyl)phthalazin-1(2*H*)-one (5c): Grey colour solid; yield: 77%, m.p.: 128-130 ºC. ^{1}H NMR (DMSO-d_6, 500 MHz) δ ppm: 1.63 (t, 3H, *J* = 10.2 Hz, CH_3), 2.68 (q, 2H, *J* = 10.8 Hz, CH_2), 2.86 (s, 3H, $ArCH_3$), 4.33 (s, 2H, NCH_2), 4.69 (s, 2H, SCH_2), 5.25 (s, 2H, NCH_2), 7.12 (d, 2H, *J* = 9.4 Hz, Ar-H), 7.18 (d, 2H, *J* = 9.4 Hz, Ar-H), 7.50 (s, 1H, triazole-H), 7.60 (t, 1H, *J* = 10.2 Hz, Ar-H), 7.70 (t, 1H, *J* = 10.2 Hz, Ar-H), 8.01 (d, 1H, *J* = 9.6 Hz, Ar-H), 8.09 (d, 1H, *J* = 9.6 Hz, Ar-H). ^{13}C NMR (DMSO-d_6, 125 MHz) δ ppm: 19.46 (CH_3), 21.47 (CH_3), 32.06 (CH_2), 36.59 (SCH_2), 51.58 (NCH_2), 55.48 (NCH_2), 118.70, 121.77, 124.28, 125.03, 128.30, 130.55, 134.09, 138.14, 140.46, 147.17, 159.81, 161.52 (oxadiazole-C), 163.56 (CO); IR (KBr, ν_{max}, cm^{-1}): 1184.14 (COC), 1241.04 (CSC), 1346.43 (N-N), 1478.30 (C=N), 1586.38 (C=C), 1641.67 (CO), 2931.05 (CH), 3017.46 (=CH). Mass (*m/z*): 474.13 $[M + H]^+$. Elemental analysis of $C_{24}H_{23}N_7O_2S$: Calcd. (found) %: C, 60.87 (60.73); H, 4.90 (4.74); N, 20.70 (20.62); S, 6.77 (6.61).

2-((5-(((1-Benzyl-1*H*-1,2,3-triazol-4-yl)methyl)thio)-1,3,4-oxadiazol-2-yl)methyl)-4-ethylphthalazin-1(2*H*)-one (5d): Gummy solid; yield: 71%, m.p.: 115-117 ºC. ^{1}H NMR (DMSO-d_6, 500 MHz) δ ppm: 1.75 (t, 3H, *J* = 10.2 Hz, CH_3), 2.30 (q, 2H, *J* = 10.8 Hz, CH_2), 4.38 (s, 2H, NCH_2), 4.80 (s, 2H, SCH_2), 5.37 (s, 2H, NCH_2), 7.16 (m, 2H, Ar-H), 7.30 (m, 3H, Ar-H), 7.37 (s, 1H, triazole-H), 7.61 (t, 1H, *J* = 10.2 Hz, Ar-H), 7.69 (t, 1H, *J* = 10.2 Hz, Ar-H), 8.03 (d, 1H, *J* = 9.6 Hz, Ar-H), 8.12 (d, 1H, *J* = 9.6 Hz, Ar-H). ^{13}C NMR (DMSO-d_6, 125 MHz) δ ppm: 14.03 (CH_3), 32.16 (CH_2), 35.90 (SCH_2), 50.04 (NCH_2), 56.39 (NCH_2), 118.42, 120.68, 126.96, 128.48, 130.31, 131.50, 134.21, 137.34, 139.35, 140.52, 144.51, 161.83, 163.68 (oxadiazole-C), 167.51 (CO). IR (KBr, ν_{max}, cm^{-1}): 1175.35 (COC), 1242.07 (CSC), 1349.29 (N-N), 1414.72 (C=N), 1514.06 (C=C), 1644.24 (CO), 2947.10 (CH), 3078.76 (=CH). Mass (*m/z*): 460.07 $[M + H]^+$. Elemental analysis: Calcd. (found) %: C, 60.12 (60.01); H, 4.61 (4.54); N, 21.34 (21.21); S, 6.98 (6.83).

4-Ethyl-2-((5-(((1-(pyridin-2-ylmethyl)-1*H*-1,2,3-triazol-4-yl)methyl)thio)-1,3,4-oxadiazol-2-yl)methyl)phthalazin-1(2*H*)-one (5e): Dark brown solid; yield: 73%, m.p.: 132-134 ºC. ^{1}H NMR (DMSO-d_6, 500 MHz) δ ppm: 1.62 (t, 3H, *J* = 10.2 Hz, CH_3), 2.28 (q, 2H, *J* = 10.8 Hz, CH_2), 4.03 (s, 2H, NCH_2), 4.65 (s, 2H, SCH_2), 5.44 (s, 2H, NCH_2), 7.20 (d, 2H, *J* = 9.4 Hz, Ar-H), 7.35 (s, 1H, triazole-H), 7.55 (m, 1H, Ar-H), 7.64 (m, 1H, Ar-H), 7.89 (d, 1H, *J* = 9.6 Hz, Ar-H), 8.09 (d, 1H, *J* = 9.6 Hz, Ar-H), 8.50 (d, 1H, *J* = 9.6 Hz, Ar-H); ^{13}C NMR (DMSO-d_6, 125 MHz) δ ppm: 14.28 (CH_3), 32.31 (CH_2), 34.46 (SCH_2), 51.44 (NCH_2), 58.18 (NCH_2), 124.77, 126.06, 128.19, 128.78, 130.21, 134.55, 136.82, 138.95, 147.82, 150.77, 151.39, 156.30, 160.55 (oxadiazole-C), 165.20 (CO). IR (KBr, ν_{max}, cm^{-1}): 1185.07 (COC), 1248.00 (CSC), 1336.58 (N-N), 1479.30 (C=N), 1512.16 (C=C), 1640.24 (CO), 2982.67 (CH), 3077.95 (=CH). Mass (*m/z*): 461.14 $[M + H]^+$. Elemental analysis of $C_{22}H_{20}N_8O_2S$: Calcd. (found) %: C, 57.38 (57.25); H, 4.38 (4.20); N, 24.33 (24.17); S, 6.96 (6.76).

General procedure for the synthesis of compounds 6a-f: Suspended 2,6-dimethylaniline (1.8 g, 14.8 mmol) in methylene chloride (25 mL) and triethylamine (2.1 g, 20.8 mmol, 1.4 equiv.) were mixed and then 2-chloroacetyl chloride (1.9 g, 17.8 mmol, 1.2 equiv.) was added dropwise in a chilled ice bath. When 2-chloroacetyl chloride was fully added, Et_3N was added if necessary to bring the pH of the reaction mixture to 8. For 3 h, the reaction mixture was stirred while being heated to reflux temperature. The organic layer was then separated, dried over Na_2SO_4 and the solvent evaporated under vacuum after it had been cleaned with a saturated citric acid solution to obtain an acidic pH. In order to obtain **6a**, a dark yellow solid with a 90% yield, the resultant residue was redissolved in DCM and purified using flash chromatography on silica gel (eluent–methanol: DCM 1:25). The same methodology was used to synthesize the remaining azide compounds (**6b-f**) and used in the next step without purification.

General procedure for the synthesis of 7a-f: Dropwise addition of K_2CO_3 (0.9 g, 7.8 mmol, 1.5 eq.) in acetone (20 mL) at 0 ºC were mixed to a solution of 1,3,4-oxadiazole (**2**, 1.5 g, 5.2 mmol). Overnight, the reaction mixture was agitated at room temperature. TLC (EtOAc:hexane) was used to monitor the resultant solution. Once the reaction was complete, dilute HCl was used to get the pH down to 3 and the reaction mixture was agitated for 1 h. Using an EtOAc:hexane (2:98) mixture as the eluent, the separated material was recovered by filtration and refined by column chromatography to yield **7a**. The remaining oxadiazoles **7b-f** were synthesized according to the procedure discussed above and these substances were purified by column chromatography using an EtOAc:hexane (20: 80). (**Scheme-II**).

N-(2,6-Dimethylphenyl)-2-((5-((4-ethyl-1-oxophthalazin-2(1*H*)-yl)methyl)-1,3,4-oxadiazol-2-yl)thio)acetamide (7a): Brown solid; yield: 76%, m.p.: 140-142 ºC. ^{1}H NMR (DMSO-d_6, 500 MHz) δ ppm: 1.79 (t, 3H, *J* = 10.2 Hz, CH_3), 2.16 (s, 6H, 2 × CH_3), 2.32 (q, 2H, *J* = 10.8 Hz, CH_2), 4.13 (s, 2H, SCH_2), 4.62 (s, 2H, NCH_2), 7.10 (t, 1H, *J* = 10.2 Hz, Ar-H), 7.17 (d, 2H, *J* = 9.4 Hz, Ar-H), 7.53 (t, 1H, *J* = 10.2 Hz, Ar-H), 7.62 (t, 1H, *J* = 10.2 Hz, Ar-H), 7.97 (d, 1H, *J* = 9.6 Hz, Ar-H), 8.20 (d, 1H, *J* = 9.6 Hz, Ar-H), 9.20 (s, 1H, NH); ^{13}C NMR (DMSO-d_6, 125 MHz) δ ppm: 15.67 (CH_3), 20.24 (CH_3), 34.19 (CH_2), 36.74 (SCH_2), 52.82 (NCH_2), 120.77, 126.09, 128.75, 130.01, 130.83, 132,43, 133,47, 134.93, 139.36, 140.03, 148.14, 161.18 (NCO), 163.42 (oxadiazole-C), 167.21 (NHCO). IR (KBr, ν_{max}, cm^{-1}): 1176.50 (COC), 1255.57 (CSC), 1341.29 (N-N), 1519.80 (C=C), 1643.24 (CO), 1727.31 (CO), 2808.16, 2990.17 (CH), 3084.90 (=CH), 3451.41 (NH). Mass (*m/z*): 450.06 $[M + H]^+$. Elemental analysis of $C_{23}H_{23}N_5O_3S$: Calcd. (found) %: C, 61.45 (61.33); H, 5.16 (5.04); N, 15.58 (15.42); S, 7.13 (7.01).

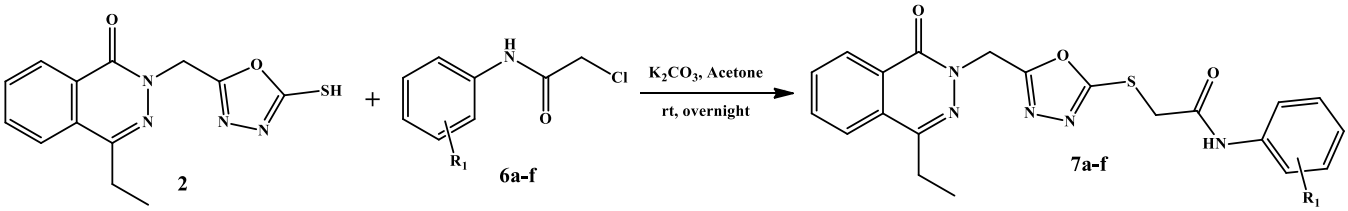

Scheme-II: Synthesis of novel 1,3,4-oxadiazole linked to acetamides (**7a-f**)

N-Benzyl-2-((5-((4-ethyl-1-oxophthalazin-2(1*H*)-yl)-methyl)-1,3,4-oxadiazol-2-yl)thio)acetamide (7b): White solid; yield: 70%, m.p.: 123-125 ºC. ^{1}H NMR (DMSO-d_6, 500 MHz) δ ppm: 1.18 (t, 3H, *J* = 10.2 Hz, CH_3), 2.13 (q, 2H, *J* = 10.8 Hz, CH_2), 3.80 (s, 2H, NCH_2), 4.13 (s, 2H, SCH_2), 4.61 (s, 2H, NCH_2), 7.19 (m, 2H, Ar-H), 7.27 (m, 3H, Ar-H), 7.69 (t, 1H, *J* = 10.2 Hz, Ar-H), 7.75 (t, 1H, *J* = 10.2 Hz, Ar-H), 8.01 (d, 1H, *J* = 9.6 Hz, Ar-H), 8.16 (d, 1H, *J* = 9.6 Hz, Ar-H), 9.38 (s, 1H, NH); ^{13}C NMR (DMSO-d_6, 125 MHz) δ ppm: 14.32 (CH_3), 31.46 (CH_2), 35.31 (SCH_2), 44.14 (NCH_2), 51.42 (NCH_2), 118.74, 120.70, 126.77, 128.24, 128.70, 129.97, 130.84, 133.99, 139.34, 139.96, 140.30, 148.20, 161.47 (NCO), 163.70 (oxadiazole-C), 167.33 (NHCO). IR (KBr, ν_{max}, cm^{-1}): 1170.71 (COC), 1275.79 (CSC), 1341.36 (N-N), 1514.02, 1602.81 (C=C), 1650.67 (CO), 1707.81 (CO), 2914.01 (CH), 3025.10 (=CH), 3337.05 (NH). Mass (*m/z*): 436.27 [M + H]$^+$. Elemental analysis of $C_{22}H_{21}N_5O_3S$: Calcd. (found) %: C, 60.68 (60.54); H, 4.86 (4.74); N, 16.08 (15.96); S, 7.36 (7.22).

2-((5-((4-Ethyl-1-oxophthalazin-2(1*H*)-yl)methyl)-1,3,4-oxadiazol-2-yl)thio)-N-(4-nitrophenyl)acetamide (7c): Yellow solid; yield: 89%, m.p.: 145-147 ºC. ^{1}H NMR (DMSO-d_6, 500 MHz) δ ppm: 1.81 (t, 3H, *J* = 10.2 Hz, CH_3), 2.38 (q, 2H, *J* = 10.8 Hz, CH_2), 4.25 (s, 2H, SCH_2), 4.75 (s, 2H, NCH_2), 7.44 (t, 1H, *J* = 10.2 Hz, Ar-H), 7.59 (t, 1H, *J* = 10.2 Hz, Ar-H), 7.75 (d, 2H, *J* = 9.4 Hz, Ar-H), 7.85 (d, 1H, *J* = 9.6 Hz, Ar-H), 8.03 (d, 1H, *J* = 9.6 Hz, Ar-H), 8.18 (d, 2H, *J* = 9.4 Hz, Ar-H), 10.01 (s, 1H, NH). ^{13}C NMR (DMSO-d_6, 125 MHz) δ ppm: 15.71 (CH_3), 31.41 (CH_2), 36.47 (SCH_2), 58.58 (NCH_2), 120.85, 121.35, 121.77, 125.16, 126.67, 130.25, 131.03, 138.36, 139.14, 140.49, 146.33, 161.41 (NCO), 164.02 (oxadiazole-C), 167.13 (NHCO); IR (KBr, ν_{max}, cm^{-1}): 1176.50 (COC), 1252.50 (CSC), 1342.31 (N-N), 1600.81 (C=C), 1641.24 (CO), 1728.17 (CO), 2811.95 (CH), 3008.03 (=CH), 3414.70 (NH). Mass (*m/z*): 467.47 [M + H]$^+$. Elemental analysis of $C_{21}H_{18}N_6O_5S$: calcd. (found) %: C, 54.16 (54.07); H, 3.95 (3.89); N, 18.14 (18.02); S, 6.98 (6.87).

N-(3-Bromo-4-methylphenyl)-2-((5-((4-ethyl-1-oxo-phthalazin-2(1*H*)-yl)methyl)-1,3,4-oxadiazol-2-yl)thio)-acetamide (7d): Brown solid; yield: 93%, m.p.: 150-152 ºC. ^{1}H NMR (DMSO-d_6, 500 MHz) δ ppm: 1.53 (t, 3H, *J* = 10.2 Hz, CH_3), 2.36 (q, 2H, *J* = 10.8 Hz, CH_2), 2.77 (s, 3H, $ArCH_3$), 4.35 (s, 2H, SCH_2), 4.63 (s, 2H, NCH_2), 7.27 (d, 1H, *J* = 9.6 Hz, Ar-H), 7.45 (d, 1H, *J* = 9.6 Hz, Ar-H), 7.61 (s, 1H, Ar-H), 7.69 (t, 1H, *J* = 10.2 Hz, Ar-H), 7.81 (t, 1H, *J* = 10.2 Hz, Ar-H), 8.01 (d, 1H, *J* = 9.6 Hz, Ar-H), 8.12 (d, 1H, *J* = 9.6 Hz, Ar-H), 10.12 (s, 1H, NH); ^{13}C NMR (DMSO-d_6, 125 MHz) δ ppm: 16.46 (CH_3), 23.87 (CH_3), 33.61 (CH_2), 37.45 (SCH_2), 52.16 (NCH_2), 120.25, 124.97, 125.69, 128.37, 128.63, 129.12, 129.61, 129.95, 134.63, 136.90, 140.12, 147.77, 161.50 (NCO), 163.93 (oxadiazole-C), 166.77 (NHCO). IR (KBr, ν_{max}, cm^{-1}): 1176.50 (COC), 1253.64 (CSC), 1351.08 (N-N), 1519.80 (C=C), 1664.38 (CO), 1720.17 (CO), 2813.95 (CH), 3082.71 (=CH), 3455.34 (NH). Mass (*m/z*): 513.51 [M]$^+$, 515.42 [M + 2H]$^+$. Elemental analysis of $C_{22}H_{20}BrN_5O_3S$: Calcd. (found) %: C, 51.48 (51.37); H, 3.99 (3.92); Br, 15.71 (15.53); N, 13.74 (13.61); S, 6.35 (6.23).

2-((5-((4-Ethyl-1-oxophthalazin-2(1*H*)-yl)methyl)-1,3,4-oxadiazol-2-yl)thio)-N-(4-methoxyphenyl)acetamide (7e): Light grey colour solid; yield: 85%, m.p.: 127-129 ºC. ^{1}H NMR (DMSO-d_6, 500 MHz) δ ppm: 1.62 (t, 3H, *J* = 10.2 Hz, CH_3), 2.30 (q, 2H, *J* = 10.8 Hz, CH_2), 3.76 (s, 3H, $ArOCH_3$), 4.40 (s, 2H, SCH_2), 4.67 (s, 2H, NCH_2), 6.92 (d, 2H, *J* = 9.4 Hz, Ar-H), 7.31 (d, 2H, *J* = 9.4 Hz, Ar-H), 7.57 (t, 1H, *J* = 10.2 Hz, Ar-H), 7.64 (t, 1H, *J* = 10.2 Hz, Ar-H), 8.05 (d, 1H, *J* = 9.6 Hz, Ar-H), 8.17 (d, 1H, *J* = 9.6 Hz, Ar-H), 10.09 (s, 1H, NH); ^{13}C NMR (DMSO-d_6, 125 MHz) δ ppm: 14.23 (CH_3), 32.55 (CH_2), 37.28 (SCH_2), 52.17 (NCH_2), 56.70 (OCH_3), 118.35, 123.77, 125.60, 127.62, 129.15, 130.10, 131.51, 131.26, 132.45, 134.65, 136.31, 146.62, 162.61 (NCO), 164.02 (oxadiazole-C), 166.41 (NHCO). IR (KBr, ν_{max}, cm^{-1}): 1176.57 (COC), 1256.64 (CSC), 1357.08 (N-N), 1600.81 (C=C), 1667.38 (CO), 1722.12 (CO), 2819.95 (CH), 3083.75 (=CH), 3453.32 (NH). Mass (*m/z*): 452.40 [M + H]$^+$. Elemental analysis of $C_{22}H_{21}N_5O_4S$: Calcd. (found) %: C, 58.69 (58.53); H, 4.83 (4.69); N, 15.70 (15.51); S, 7.21 (7.10).

2-((5-((4-Ethyl-1-oxophthalazin-2(1*H*)-yl)methyl)-1,3,4-oxadiazol-2-yl)thio)-N-(*p*-tolyl)acetamide (7f): White colour solid; yield: 82%, m.p.: 130-132 ºC. ^{1}H NMR (DMSO-d_6, 500 MHz) δ ppm: 1.75 (t, 3H, *J* = 10.2 Hz, CH_3), 2.33 (q, 2H, *J* = 10.8 Hz, CH_2), 2.80 (s, 3H, $ArCH_3$), 4.11 (s, 2H, SCH_2), 4.37 (s, 2H, NCH_2), 7.12 (d, 2H, *J* = 9.4 Hz, Ar-H), 7.37 (d, 2H, *J* = 9.4 Hz, Ar-H), 7.66 (t, 1H, *J* = 10.2 Hz, Ar-H), 7.80 (t, 1H, *J* = 10.2 Hz, Ar-H), 7.91 (d, 1H, *J* = 9.6 Hz, Ar-H), 8.13 (d, 1H, *J* = 9.6 Hz, Ar-H), 10.12 (s, 1H, NH); ^{13}C NMR (DMSO-d_6, 125 MHz) δ ppm: 15.69 (CH_3), 21.40 (CH_3), 33.31 (CH_2), 37.11 (SCH_2), 51.49 (NCH_2), 124.92, 125.65, 128.68, 128.91, 129.04, 130.17, 131.50, 131.73, 132.94, 134.61, 136.37, 147.76, 161.64 (NCO), 163.70 (oxadiazole-C), 166.77 (NHCO); IR (KBr, ν_{max}, cm^{-1}): 1184.21 (COC), 1243.00 (CSC), 1342.36 (N-N), 1476.30 (C=N), 1585.38 (C=C), 1631.67 (CO), 1686.67 (CO), 2931.67 (CH), 3013.53 (=CH), 3275.05 (NH). Mass (*m/z*): 436.25 [M + H]$^+$. Elemental analysis of $C_{22}H_{21}N_5O_3S$: Calcd. (found) %: C, 60.81 (60.68); H, 4.94 (4.86); N, 16.20 (16.08); S, 7.48 (7.36).

Antimicrobial activity: The investigation into the antimicrobial efficacy of the examined compounds utilized

the agar well diffusion method [37,38]. An *in vitro* assay was conducted to evaluate the antibacterial activity of a compound (15 mg/mL) against Gram-positive bacteria (*Bacillus subtilis*, *Staphylococcus aureus*) and Gram-negative bacteria (*Escherichia coli*, *Klebsiella pneumoniae*), using nutrient agar medium. Antifungal activity was tested against *Aspergillus flavus* and *Candida albicans* on Sabouraud dextrose agar. Microbial strains were obstained from IMTECH (MTCC), Chandigarh, India. Levofloxacin and clotrimazole served as standard drugs for antibacterial and antifungal assays, respectively, while DMSO was used as the negative control.

Testing method: Aseptically prepared culture media (20-25 mL) were poured into Petri dishes and allowed to solidify at room temperature. A microbial suspension (1.5×10^5 CFU/mL), adjusted to 0.13 $OD_{625\ nm}$ (McFarland 0.5 standard), was prepared in sterile saline. Within 15 min, sterile cotton swabs were dipped into the suspension and evenly spread onto the agar surface. After a 15 min rest period, 6 mm wells were created using a sterile borer, and 100 µL of test compound was added to each well. Plates were incubated at 37 ºC for 24 h to evaluate the antibacterial activity. All tests were performed in triplicate and inhibition zone diameters were measured in millimeters, following a previously reported method.

Molecular docking studies: The *in silico* molecular docking study was carried out using the Autodock 4.2. Protein preparation was carried out by Autodock Tools. Ligand preparation and grid generation were carried out by Autodock 4.2. Receptor-ligand docking was carried out by Autodock.

Selection of target protein and preparation of protein target structure: The crystal structure of *E. coli* topoisomerase IV pare 24kda subunit, whose PDB ID is 1S14 and the 3.5 A crystal structure of the catalytic core (B'A' region) of *S. aureus* DNA Gyrase complexed with GSK299423 and DNA, whose PDB ID is 2XCR were retrieved from the PDB (Protein Data Bank) and used for molecular docking. 1S14 seems to have a 2.00 Å resolution and one 194-amino-acid-residue protein of chain A. The molecular weight of the protein is 21702.42 kDa and 2XCR seems to have a 3.50 Å resolution and one 726-amino-acid-residue protein of chain A. The molecular weight of the protein is 82216.94 kDa. Autodock Tools (ADT) 1.5.6 was used to prepare the input files. Hetero atom *i.e.*, novobiocin have been removed completely and also removed water molecules. All hydrogens were added and saved it in pdbqt format.

Selection and preparation of ligand molecules: One synthesized molecule used in this study. The molecule was sketched in Tripos sybyl6.7 and minimized by using Gasteiger-Hückel charges and saved it in .mol2 format. All Ligands being uploaded individually in .mol2 format into the Autodock Tools and torsion angles were set and saved it in PDBQT format.

Molecular docking analysis: The proteins and ligand were uploaded individually and removed water molecules and added all hydrogens. Later the protein was saved in pdbqt format. The standard docking procedure was employed for a rigid protein and a flexible ligand whose torsion angles were identified. Active site was predicted using PDBsum. Grid dimensions selected as 60, 60 and 60 points and the amino acids, which are present in the active site were selected and centred the in x, y and z directions was built with a grid spacing of 0.375 Å and a distance-dependent function of the dielectric constant were used for the calculation of the energetic map. Lamarckian genetic algorithm method was employed for docking simulations [39-41]. At the end of docking, the best poses were analysed for hydrogen bonding calculations using Autodock 4.2, Ligplot plus and Biovia Discovery studio visualizer from the estimated free energy of ligand binding (ΔG binding, kcal/mol), the inhibition constant (K_i) for each ligand was calculated.

RESULTS AND DISCUSSION

This work is the continuation of previous work reported on the synthesis and docking studies of 1,3,4-oxadiazole derivatives [42]. Two different synthetic approaches were adopted for the synthesis of 4-ethyl-2-((5-mercapto-1,3,4-oxadiazol-2-yl)methyl)phthalazin-1(2*H*)-one scaffold (**Schemes I** and **II**). The key starting material 2-(4-ethyl-1-oxophthalazin-2-(1*H*)-yl) acetohydrazide (**1**) was afforded *via* the mixture of ethyl 2-(4-ethyl-1-oxophthalazin-2(1*H*)-yl)acetate and hydrazine hydrate (1:1) in ethanol at reflux.

In the first approach, the synthesis began with the reaction of 2-(4-ethyl-1-oxophthalazin-2(1*H*)-yl)acetohydrazide (**1**), KOH and CS_2 in ethanol at 60 ºC for 10 h. The solvent was evaporated, the obtained residue was poured on crushed ice and acidified with dil. HCl till a pH of 5. The crude product was filtered out, cleaned with water, dried and recrystallized from ethanol to obtain the key intermediate **2** as pale-yellow solid with 81% yield. To synthesis oxophthalazin-1,3,4-oxadiazole hybrid **3**, compound **2** was treated with propargyl bromide and $NaHCO_3$ in DMF at 90 ºC to obtain propargylated 1,3,4-oxadiazole (**3**) in high yield [35]. To synthesize the desired library of substituted triazoles, we envisioned utilizing a click chemistry approach, specifically the copper catalyzed azide–alkyne cycloaddition (CuAAC), due to its efficiency, reliability and regioselectivity. Different azides, intermediates **4a-e**, were prepared by the reaction of corresponding amines, sodium nitrate in acetic acid in good yield (80-90%) [36]. Further the substituted azides were treated with 4-ethyl-2-((5-(prop-2-yn-1-ylthio)-1,3,4-oxadiazol-2-yl)methyl)phthalazin-1(2*H*)-one (**3**), sodium ascorbate, copper sulphate to obtain corresponding oxophthalazine-triazole-oxadiazole **5a-e** in excellent yield.

In second approach, the synthesis of target compounds **7a-f** began with the formation of 2-chloro-N-(2,6-dimethylphenyl)acetamide (**6a**) by the reaction of 2,6-dimethylaniline with 2-chloroacetyl chloride, TEA in DCM at 0 ºC. Compound **6a** was subsequently treated with compound **2** in acetone/K_2CO_3 at room temperature to obtain crude *N*-(2,6-dimethylphenyl)-2-((5-((4-ethyl-1-oxophthalazin-2(1*H*)-yl)methyl)-1,3,4-oxadiazol-2-yl)thio)acetamide (**7a**). The pure desired product was obtained by column chromatography using EtOAc:hexane (20: 80) as eluent (**Scheme-II**). Other 1,3,4-oxadiazoles **7b-f** were also produced using the same synthetic approach.

All the final compounds were thoroughly characterized by using Mass, FT-IR, ^1H and ^{13}C NMR spectroscopy techniques. The FTIR analysis of compound **5a** showed the charac-

teristic bands for conjugated C=O and C=C absorptions at 1638.67 and 1587.38 cm^{-1}, aromatic =CH at 3055.39 cm^{-1} and aliphatic -CH stretching frequency at 2924.76 cm^{-1}, respectively. Furthermore, the N-N functionality was confirmed by the stretching frequency at 1345.36 cm^{-1}, whereas the COC and CSC stretching were seen at 1193.85 and 1248.00 cm^{-1}, respectively. The ^1H NMR spectra of compound **5a** at δ 7.46 ppm as a singlet confirmed presence of olefinic proton of the triazole ring. The methylene protons adjacent to the triazole (NCH_2), oxadiazole (SCH_2) and phthalazine (NCH_2) skeleton were detected at δ 5.42, 4.74 and 4.29 ppm, respectively. The phenylic protons phthalazine ring were observed at δ 7.27 and 8.19 ppm having coupling constant of J = 9.4 Hz for the *para* coupling. The methylene protons were observed at δ 1.64 as quartet and the methyl protons were observed at 2.23 ppm as triplet showed the presence of ethyl group and the protons between δ 7.37-8.28 ppm confirmed the aromatic functionalities. Further the ^{13}C NMR spectra substantiated the presence of triazole and oxadiazole ring carbons at δ 161.42, 148.13 ppm and carbonyl group of phthalazine moiety carbon at δ 164.02 ppm. The chemical shift values of aromatic carbons ranging between δ 144.49-120.89 ppm and the chemical shift values of the methylene carbons in n-linker and s-linker carbons appears between δ 59.14-36.47 ppm, which gives the distinctive properties for the synthesis of the corresponding 1,3,4-oxadiazole substituted 1,2,3-triazole product **5a**. Finally, the recorded mass *m/z* at (505.32 $[M + H]^+$), which is in agreement with the expected formula $C_{23}H_{20}N_8O_4S$.

Similarly, the structures of compounds **7a-f** were confirmed by detailed NMR, Mass and FTIR analysis. The FTIR analysis of **7a** showed amide N-H stretching at 3451.41 cm^{-1} and two carbonyl groups of phthalazine ring and amide carbonyl groups exhibited stretching frequency at 1727.31 and 1643.24 cm^{-1}, respectively. The aromatic =CH stretching showed at 3084.90 cm^{-1} and aliphatic -CH showed at 2990.97 cm^{-1}. The C=C functions are accounted for by the stretching frequency bands in the 1599.88 to 1519.80 cm^{-1} region. In addition, the COC, CSC stretching vibration bands were observed at 1176.50, 1255.57 cm^{-1}, respectively, whereas the N-N stretching was detected at 1341.29 cm^{-1}. The ^1H NMR spectra of **7a** showed characteristic signals of the protons corresponding to the aromatic region between δ 8.20 to 7.10 ppm and the amide (NH) group showed at δ 9.20 ppm. The ^1H NMR signals at δ 4.62 and 4.13 ppm correspond to 2H were assigned to the methylene protons. In ^{13}C NMR spectra, the presence of characteristic signals between δ 167.21, 163.42 and 161.18 ppm correspond to the amide carbonyl, oxadiazole and oxophthalazinone carbons, respectively. The presence of characteristic signals between δ 148.14 to 120.77 ppm correspond to the aromatic carbons. The characteristic signals at δ 52.82, 36.74 ppm for -NCH_2, -SCH_2 and between δ 20.24 and 15.67 ppm for methylene and methyl carbons on phthalazine. Finally, the structure was validated by the high accuracy of the experimental values *m/z* = 450.06 of $[M+H]^+$ in compound **7a** mass spectra when compared to their computed ones.

Antimicrobial studies: The comparative study of the activity of the novel compounds (**5** & **7**) was carried out on bacteria, *Bacillus subtilis*, *Staphylococcus aureus*, *Escherichia coli*, *Klebsiella pneumoniae* and fungal strains, *Aspergillus flavus*, *Casndida albicans* when compared to reference drugs levofloxacin and clotrimazole. According to the zone of inhibition values (ZI), all the synthesized compounds were tested on both Gram-positive and Gram-negative bacteria at varying concentrations (0.1 to 0.5 mg/mL) formed four sub-groups. It was observed that the *in vitro* antibacterial activity of compounds **5a**, **5e**, **7a** and **7d** significantly different from all other derivatives (Table-1). It is also evident that compounds **5a**, **5e**, **7a** and **7d**, exhibited significantly high antibacterial activity against *S. aureus* with diameter zone of inhibitions of 40.24 ± 0.05, 36.82 ± 0.12, 43.01 ± 1.04 and 44.12 ± 0.05 mm and also with standard (42.05 ± 0.11 mm). Furthermore, compounds **5e** and **7a** exhibit significantly high antibacterial activity against Gram-positive bacteria *B. subtilis* with their ZI values of 33.26 ± 4.73, 36.12 ± 1.00 mm and **5c**, **7c** and **7e** are moderate to good antibacterial effect on *B. subtilis* strain (28.61 ± 0.04, 30.45 ± 0.03, 20.34 ± 0.06 mm). Moreover,

TABLE-1
ZONE OF INHIBITIONS OF TRIAZOLYL-OXADIAZOLES (**5a-e**) AND OXADIAZOLE ACETAMIDE DERIVATIVES (**7a-f**) AGAINST BACTERIAL AND FUNGAL STRAINS

Compd.	Gram-positive bacteria		Gram-negative bacteria		Fungal strains	
	B. subtilis	*S. aureus*	*E. coli*	*K. pneumonia*	*A. flavus*	*C. albicans*
5a	35.17 ± 0.18	40.24 ± 0.05	45.01 ± 0.09	28.45 ± 0.12	29.02 ± 0.20	NS
5b	19.35 ± 0.01	16.35 ± 0.04	NS	20.11 ± 0.19	18.01 ± 0.09	15.70 ± 0.07
5c	28.61 ± 0.04	24.98 ± 0.16	29.01 ± 1.01	NS	23.42 ± 0.05	26.90 ± 0.02
5d	NS	13.57 ± 0.06	11.47 ± 0.84	8.02 ± 1.10	NS	9.23 ± 0.22
5e	40.23 ± 0.07	36.82 ± 0.12	35.80 ± 1.06	36.98 ± 0.10	31.67 ± 0.27	NS
7a	36.12 ± 1.00	43.01 ± 1.04	40.04 ± 0.03	36.24 ± 0.02	30.27 ± 1.02	28.20 ± 0.06
7b	10.23 ± 0.12	NS	12.45 ± 0.14	NS	NS	9.34 ± 0.04
7c	30.45 ± 0.03	29.35 ± 1.11	25.34 ± 1.21	22.45 ± 0.06	20.23 ± 0.11	NS
7d	NS	44.12 ± 0.05	43.70 ± 0.12	36.80 ± 1.27	30.24 ± 0.14	31.56 ± 1.20
7e	20.34 ± 0.06	21.87 ± 1.01	NS	23.56 ± 0.09	24.78 ± 0.18	21.85 ± 0.10
7f	16.35 ± 0.22	NS	20.45 ± 0.25	NS	NS	18.43 ± 1.23
LVF	38.19 ± 0.02	42.05 ± 0.11	44.12 ± 1.02	35.24 ± 1.08	ND	ND
CLZ	ND	ND	ND	ND	32.17 ± 0.92	30.31 ± 0.84

LVF: Levofloxacin, CLZ: Clotrimazole; Mean of the size of the inhibition zone (mm): 35-45 (very highly significant); 25-35 (highly significant); 10-25 (significant); NS: Non-significant; ND: not done. Experiments = 3. Values = mean ± SEM.

compounds **5a**, **7a** and **7d** exhibits a significantly high anti-bacterial effect against *E. coli* strain as ZI = 45.01 ± 0.09, 40.04 ± 0.03, 43.70 ± 0.12 mm, respectively, which are most active compared to levofloxacin (LVF) (44.12 ± 1.02 mm). Screening results showed that compounds **5d** and **7b** had a less anti-bacterial activity (ZI = 11.47 ± 0.84, 12.45 ± 0.14 mm), whereas compounds **5b**, **7e** are not shown any significant active against *E. coli*. In addition, the synthesized compounds **5e**, **7a** and **7d** revealed more active on Gram-negative bacteria *K. pneumonia* with zone of inhibition values 36.98 ± 0.10, 36.24 ± 0.02, 36.80 ± 1.27 mm, respectively and these are highest activity than LVF (35.24 ± 1.08 mm). These activities decrease in the compounds **5b**, **7c** and **7e** on *K. pneumonia* (ZI = 20.11 ± 0.19, 22.45 ± 0.06, 23.56 ± 0.09 mm) and compounds **5c**, **7b** and **7f** had no activity on *K. pneumonia*.

Compound **5e**, **7a** and **7d** having 2-pyridinyl, *o*-dimethyl phenyl, bromo-methyl phenyl functionality was more active against *A. flavus* (31.67 ± 0.27, 30.27 ± 1.02, 30.24 ± 0.14 mm) than clotrimazole (32.17 ± 0.92 mm). 1,2,3-Triazole with *p*-substituents such as nitrophenyl (**5a**; 29.02 ± 0.20 mm) and methoxyphenyl (**5b**; 18.01 ± 0.09 mm) and methyl phenyl (**5c**; 23.42 ± 0.05 mm) exhibited moderate activity, while the other compounds **5d**, **7b** and **7f** had no activity on on *A. flavus*. Compound with electron-donating groups such as *p*-Me (**5c**) and groups such as *o*-diMe (**7a**), *p*-Me, *m*-Br (**7d**) displayed appreciable activity on *C. albicans* (26.90 ± 0.02, 28.20 ± 0.06, 31.56 ± 1.20 mm, respectively). However, the electron-donating groups like *p*-Me (**5c**) and moderate electron-donating groups like *p*-OMe (**7e**) exhibited antifungal activity against *C. albicans*. Extended heterocyclic conjugations without substituent on the phenyl ring (compounds **5d**, **7b**; 9.23 ± 0.22, 9.34 ± 0.04 mm) gave low activity. With the highest zone of inhibition values, nitrogen-rich compounds like **5d** and **7b** showed superior antibacterial activity. In order for the molecules to precisely interact with the target bacterial and fungal strains, they may have additional hydrogen bond-acceptors. Therefore, in this study, compounds **5a**, **5e**, **7a** and **7d** are identified as the most effective agents against both bacteria and fungi.

Docking results: Through their mechanism of action, the docking investigation examined the antibacterial characteristics of the newly synthesized compounds phthalazin-1(2*H*)-one carrying 1,3,4-oxadiazole and 1,2,3-triazole derivatives (**5a**, **7a** and **7d**). To ascertain the most likely mechanism of anti-bacterial action of the most active synthesized compounds to bind with DNA gyrase and Topoisomerase-IV (PDB IDs: 2XCR and 1S14), molecular docking was employed [43-47]. The protein–ligand interaction behaviour were estimated using binding interactions. Figs. 2-4 provide a thorough explanation of the kind of interaction and the interacting amino acid residues. Since it causes negative supercoiling, which is necessary for DNA replication, transcription and recombination, bacterial DNA gyrase is crucial to the research of antibacterial drugs. However, compound **5a** exhibits two interactions: a hydrophobic pi-sulfur stacked with Met1074(A) at a distance of 2.69 Å and a Pi-anion bond with Glu1046(A) at a distance of 2.72 Å. The 1,2,3-triazole fragment has a single carbon H-bond with the Pro1075(A) residue at 2.50 Å, while it interacts with Pro1075(A) and Met1074(A) through pi-alkyl interactions. Furthermore, ligand **5a** shows two H-bond interactions between phthalazine (N9) and OG of Ser1043(A) (distance = 3.04 Å) and OD2 of Asp1069(A) (distance = 3.00 Å) and triazole (N14) exhibited two more H-bond stackings with Asp1069(A) at distance of 3.20 Å and 3.13 Å, respectively. Furthermore, the active site of *E. coli* from topoisomerase IV (PBB: 1S14) has established van der Waals interactions Arg1072(A), Asn1042(A), Ile1090(A), Ser1043(A), Ile1068 (A), Ser1164(A), Thr1163(A) and Val1039(A) in addition to alkyl-alkyl and pi-alkyl interactions with Val1067(A),

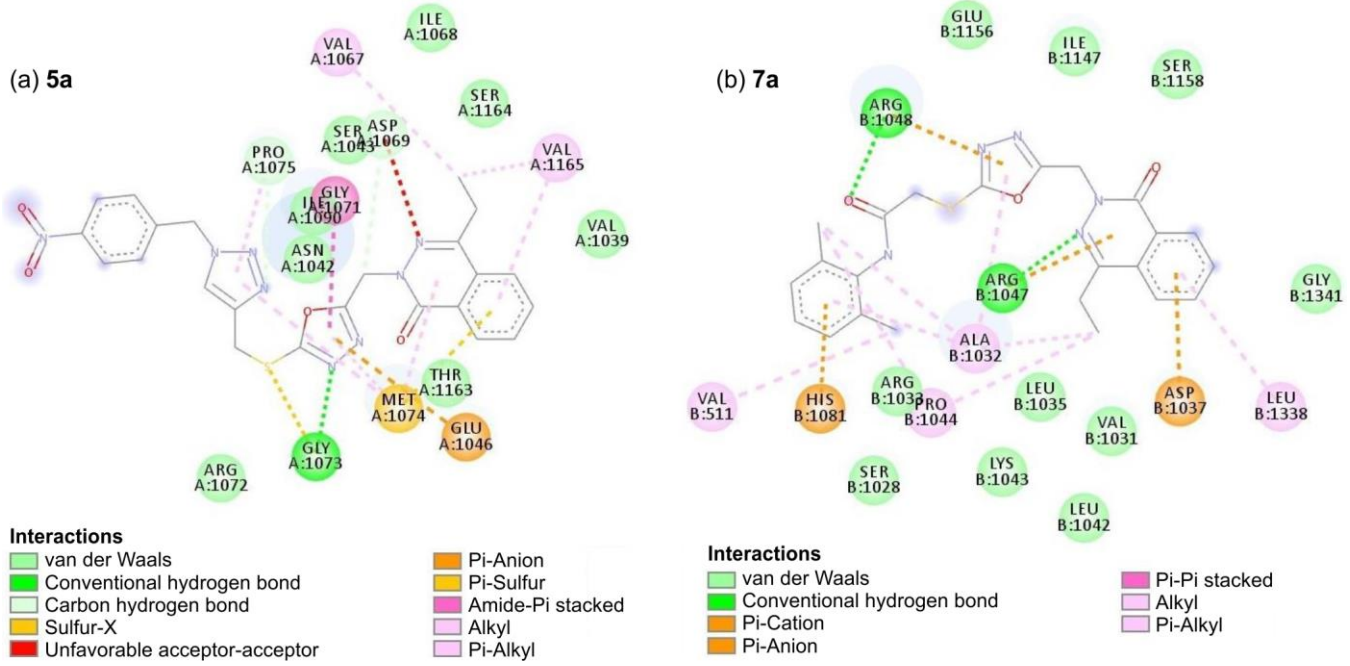

Fig. 2. (a) 2D-Surface flexibility docking image of ligand **5a** in the possible PDB binding pocket (1S14); (b) 2D-confirmation of the most active ligand **7a** against 2XCR

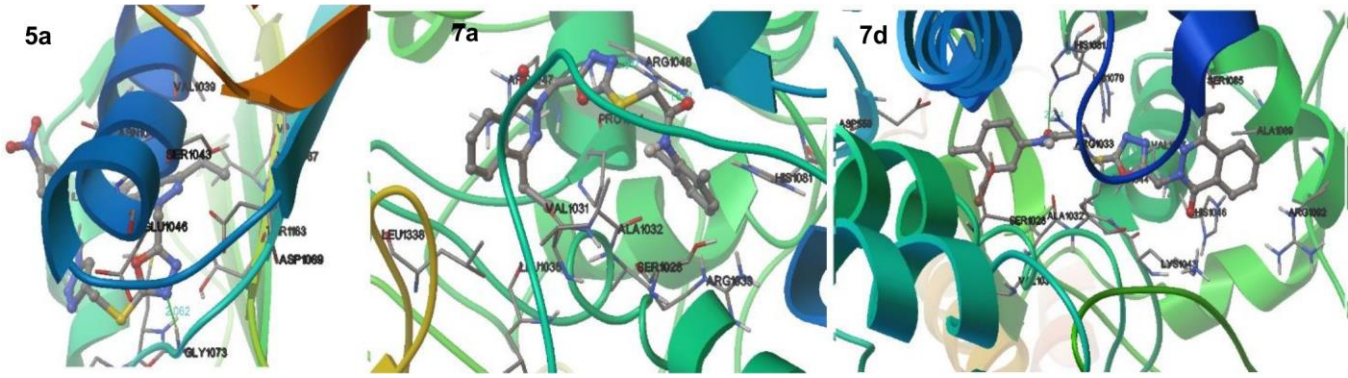

Fig. 3. 3D-Surface flexibility docking images of ligands **5a**, **7a** and **7d** against 1S14 & 2XCR protein

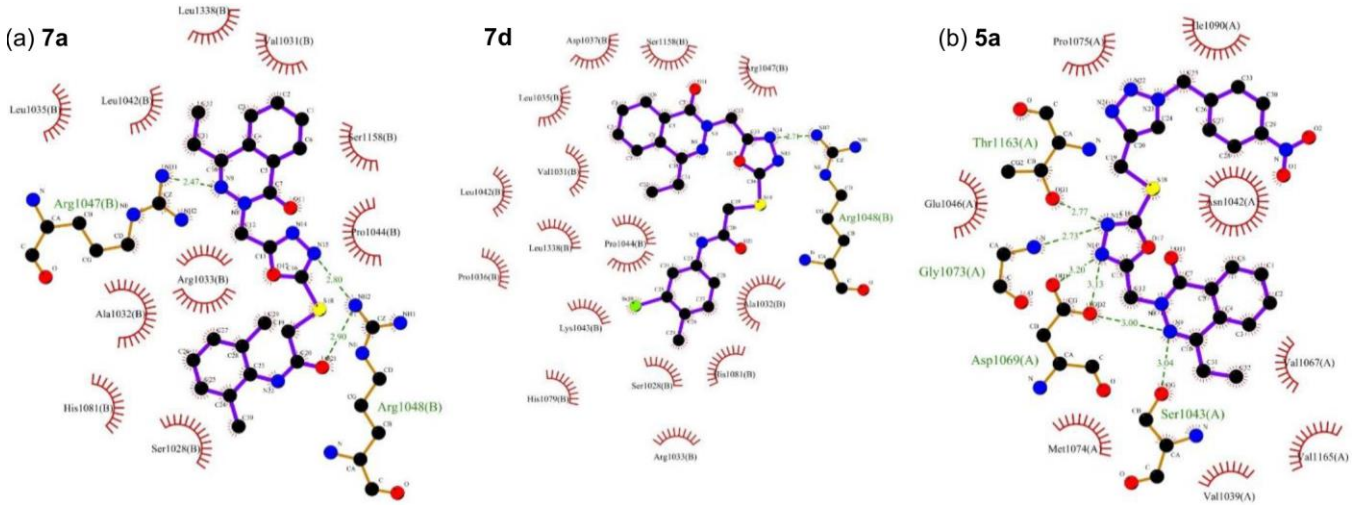

Fig. 4. (a) Ligplot confirmations of most active ligands **7a**, **7d** against 2XCR; (b) Ligplot images of **5a** against 1S14 protein

Val1165(A) × 2 and Met1074(A) × 2 (Table-2). Furthermore, there are unfavourable accepter-accepter contacts and visible substituents *via* carbon-H between the methylene system and the nitrogen's oxophthalazine ring with Asp1069(B). Moreover, at a distance of 3.35 Å, the oxadiazole ring's aromatic system interacts with Gly1071(B) pi-pi in a shaped orientation.

Compound **7a** interacted hydrophobically van der Waals interactions with Ser1028(B), Lys1043(B), Leu1042(B), Val1031 (B), Leu1035(B), Arg1033(B), Gly1341(B), Glu1156(B), Ile1147(B) and Ser1158(B). In a hydrophobic pi-cation contact, His1081(B) and Asp1037(B) establish a bond with the 2,6-dimethylphenyl and phthalazine groups of ligands **7a**. The 1,3,4-oxadiazole group and its thioacetamide interacted with Arg1048(B) residue *via* H-bonding and pi-anion with distance 2.90 Å and 3.17 Å, while its N15 atom connected *via* H-bonding with Arg1048(B) [2.80 Å]. The N9 group of oxophthalazine indicated that the H-bonding with NH1 of Arg1047(B) [2.47 Å], Arg1047(B) was involved in the hydrophobic interaction, particularly the pi-cation interaction and other amino acid residues such as Val511(B), Pro1044(B) × 2, Ala1032(B) × 4 and Leu1338(B) involved in the hydrophobic pi-alkyl, alkyl-alkyl interactions provide stability to the complex (Figs. 2 and 4). In addition, compound **7d** exhibits six interactions: two important Pi-anion bonds with Lys1043(B) and His1081(B) at distances of 3.13 Å and 2.87 Å, respectively and six van der Waal bonds with Ser1028(B), Ser1158 (B), Asp1037(B), Leu1042(B), Leu1338(B) and Pro1036(B) residues in the active site of *S. aureus* DNA gyrase complexed (PDB: 2XCR), respectively. The Arg1048(B) was found to H-bond interact with nitrogen atom from 1,3,4-oxadiazole at distance of 2.71 Å. Compounds **7a, 7d** and **5a** exhibits a good binging energy within the active site these proteins [-7.12, -6.96, -7.52 kcal/mol] and dissociation constant of 5.99, 7.96 and 3.09 μM, respectively.

Computational studies: All the compounds chemical structure affects its molecular weight (MW), number of rotational bonds (nRot), hydrogen bonding potential (nHA and nHD), aqueous solubility (logS), lipophilicity (logP), carbon bond saturation (Fsp^3), topological polar surface of the molecule (TPSA) and other structural characteristics (Table-3). As indicated in Fig. 5, the synthesized compounds are visually displayed in pink area radar plots, demonstrating an appropriate range of the parameters described previously. The first step in assessing the drug similarity of the compounds created in this work was to determine how closely the tested structures adhered to the Pfizer, Golden, GSK, Ghose and Veber guidelines developed by Lipinski. Thus, these compounds were fulfilled good medicinal chemistry and pharmacokinetics properties with satisfied criterion of drug-likeness (Table-4) [48]. The topological polar surface area (TPSA), on the other hand, is a key descriptor used to assess the ability of molecule to permeate cell membranes and is closely associated with its

TABLE-2
DOCKING POSE INTERACTIONS DATA OF THE MOST ACTIVE COMPOUNDS AGAINST ANTIBACTERIAL PROTEINS

Ligands	ΔG (kcal/mol)	K_i (μM)	Interacting amino acid residues	Bond distance (Å)
Ligand **5a** against active site of *E. coli* Topoisomerase-IV (1S14)				
5a	-7.52	3.09	**van der Waals**: Arg1072(A), Asn1042(A), Ile1090(A), Ser1043(A), Ile1068(A), Ser1164(A), Thr1163(A) and Val1039(A) **Pi-anion**: Glu1046(A) **Pi-sulfur**: Met1074(A) **Pi-alkyl & alkyl-alkyl**: Pro1075(A), Val1067(A), Val1165(A) × 2, Met1074(A) × 3 **Pi-Pi**: Gly1071(A) **H-bond**: Pro1075(A) **CH-bond**: Asp1069(A)	 2.72 2.69 3.35 2.50 2.71
Ligands **7a** and **7d** against active site of *S. aureus* DNA Gyrase (2XCR)				
7a	-7.12	5.99	**van der Waals**: Ser1028(B), Lys1043(B), Leu1042(B), Val1031(B), Leu1035(B), Arg1033(B), Gly1341(B), Glu1156(B), Ile1147(B), Ser1158(B) **Pi-cation**: His1081(B), Asp1037(B), Arg1047(B) **Pi-anion**: Arg1048(B) × 2 **H-bond:** Arg1048(B), Arg1047(B) **Pi-alkyl & alkyl-alkyl**: Val511(B), Pro1044(B) × 2, Ala1032(B) × 4, Leu1338(B)	 2.58, 2.27, 2.79 2.90, 3.17 2.80, 2.47
7d	-6.96	7.96	**van der Waals**: Ser1028(B), Ser1158(B), Asp1037(B), Leu1042(B), Leu1338(B), Pro1036(B) **Pi-anion**: Lys1043(B), His1081(B) **H-bond**: Arg1048(B)	 3.13, 2.87, 2.71

TABLE-3
PHYSICO-CHEMICAL PROPERTIES OF COMPOUNDS **5a-e** AND **7a-f**

Compd.	MF	MW	nHA	nHD	nRot	Fsp3	Np	nHet	TPSA	MCE-18	LogS	LogP
5a	$C_{23}H_{20}N_8O_4S$	504.13	12	0	9	0.21	-2.27	13	147.66	27.0	-4.25	2.73
5b	$C_{24}H_{23}N_7O_3S$	489.16	10	0	9	0.25	-2.05	11	113.75	26.0	-4.32	2.38
5c	$C_{24}H_{23}N_7O_2S$	473.16	9	0	8	0.25	-2.19	10	104.52	26.0	-4.75	3.25
5d	$C_{23}H_{21}N_7O_2S$	459.15	9	0	8	0.21	-2.14	10	104.52	25.0	-4.02	2.70
5e	$C_{22}H_{20}N_8O_2S$	460.14	10	0	8	0.22	-2.37	11	117.41	25.0	-3.13	1.69
7a	$C_{23}H_{23}N_5O_3S$	449.15	8	0	8	0.26	-2.17	9	102.91	23.0	-4.47	3.00
7b	$C_{22}H_{21}N_5O_3S$	435.14	8	1	9	0.22	-2.15	9	102.91	21.0	-4.09	2.66
7c	$C_{21}H_{18}N_6O_5S$	466.11	11	1	9	0.19	-2.43	12	146.05	23.0	-4.93	3.03
7d	$C_{22}H_{20}BrN_5O_3S$	513.05	8	1	8	0.22	-2.37	10	102.91	23.0	-5.52	4.04
7e	$C_{22}H_{21}N_5O_4S$	451.13	9	1	9	0.22	-2.2	10	112.14	22.0	-4.74	3.08
7f	$C_{22}H_{21}N_5O_3S$	435.14	8	1	8	0.22	-2.3	9	102.91	22.0	-5.07	3.53
LVF	$C_{18}H_{20}FN_3O_4$	361.37	7	1	2	0.44	-0.21	8	75.01	83.07	-2.01	-0.25

TABLE-4
MEDICINAL CHEMISTRY & PHARMACOKINETICS PROPERTIES OF COMPOUNDS **5a-e** AND **7a-f**

Molecules	Lipinski #violations	Pfizer rule	Golden rule	GSK rule	Ghose #violations	Veber #violations	Carcino-genicity	Eye Corrosion	PAINS #alerts	Synthetic Accessibility	BCRP
5a	1	0	1	1	1	1	0.71	0.0	0	2.78	$3.9xe^{-10}$
5b	0	0	0	1	1	0	0.67	0.0	0	2.68	$1.2xe^{-09}$
5c	0	0	0	1	0	1	0.55	$7.2xe^{-08}$	0	2.67	$2.3xe^{-10}$
5d	0	0	0	1	0	1	0.53	$5.4xe^{-08}$	0	2.63	$2.8xe^{-10}$
5e	0	0	0	1	1	0	0.658	$1.1xe^{-07}$	0	2.78	$1.6xe^{-10}$
7a	0	0	0	1	1	0	0.537	$1.9xe^{-07}$	0	2.47	$6.2xe^{-13}$
7b	0	0	0	1	1	0	0.380	$8.1xe^{-09}$	0	2.35	$3.1xe^{-12}$
7c	0	0	0	1	1	0	0.530	$1.9xe^{-06}$	0	2.48	$2.5xe^{-13}$
7d	0	0	0	1	1	0	0.539	$5.4xe^{-08}$	0	2.63	$2.8xe^{-10}$
7e	0	0	0	1	1	0	0.523	$3.7xe^{-08}$	0	2.36	$5.8xe^{-13}$
7f	0	0	0	1	1	0	0.382	$7.2xe^{-07}$	0	2.35	$6.3xe^{-14}$
LVF	0	0	0	0	0	0	0.598	$1.5xe^{-05}$	0	3.09	0.0008

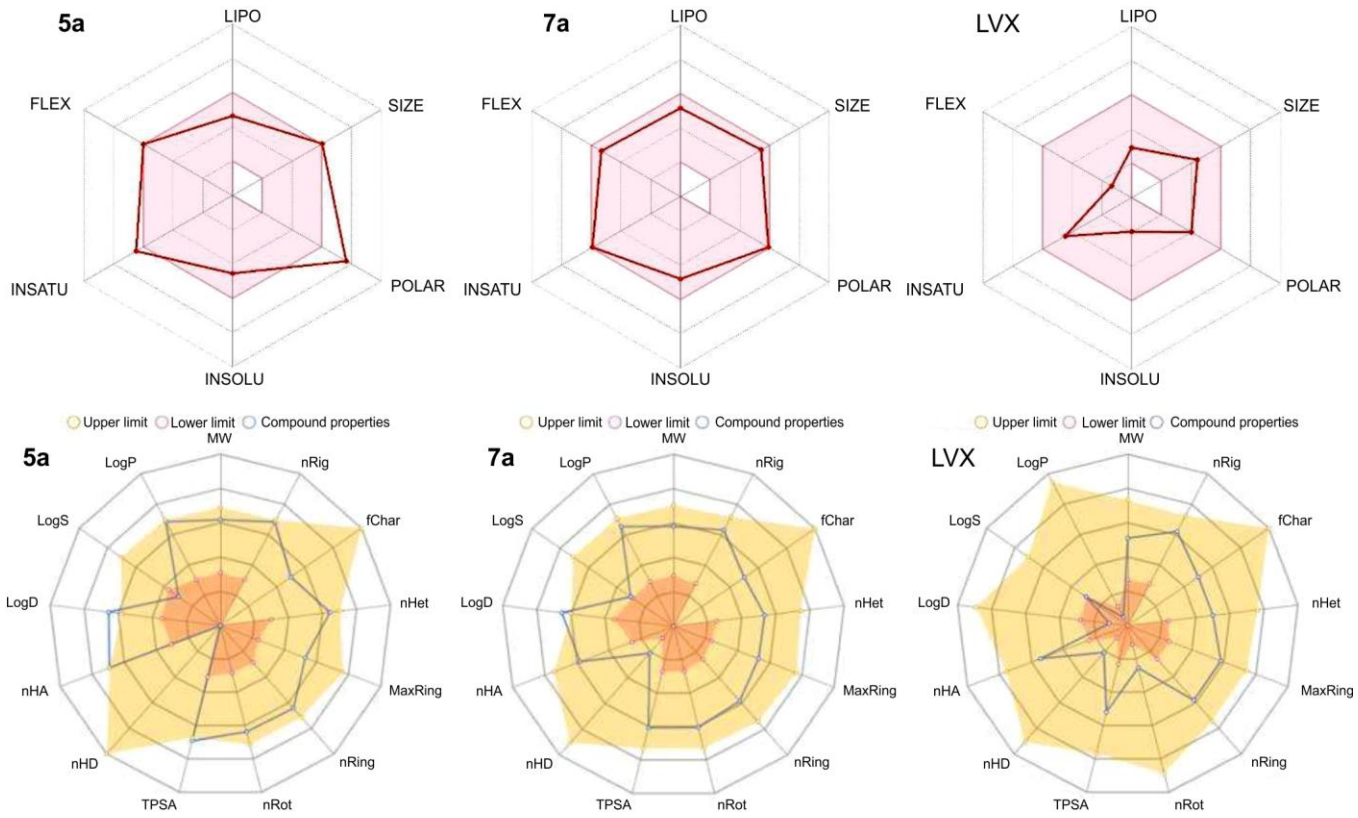

Fig. 5. Bioavailability radar platforms of compounds **5a**, **7a** and LVX

bioavailability. To guarantee adequate absorption, the TPSA for drugs taken orally should be less than 140 A^2.

The initial assessment of a drug candidate's ADME properties, along with the prediction of its potential toxicity, represents a critical step in the drug development process. Among the different parameters defining the absorption phase, the BOILED-Egg model (Fig. 6, Table-5) chose water solubility, Caco-2 permeability, absorption in the human intestine (HIA), blood-brain barrier (BBB) permeability and the potential to be a *p*-glycoprotein (P-gp) substrate and a *p*-glycoprotein inhibitor [49]. Predicting the metabolism of compound is a crucial step in the discovery of novel medicines. Cytochrome P participates in phase I processes and is associated with the biotransformation of medications. The following cytochrome P450 monooxygenase family isoforms were found to interact with the investigated compounds: CYP1A2, CYP2C9, CYP3A4, CYP2C19 and CYP2D6. The present results imply that the best-docked triazoles and oxadiazole may be a novel class of antibacterial medications since they showed appropriate pharmacokinetic, bioavailability and physio-chemical responses *in silico* without any toxicity or carcinogenicity. For the classification endpoints, the prediction probability values are transformed into six symbols: 0-0.1 (---), 0.1-0.3 (--), 0.3-0.5 (-), 0.5-0.7 (+), 0.7-0.9 (++) and 0.9-1.0 (+++).

TABLE-5
ABSORPTION, DISTRIBUTION AND TOXICITY OF COMPOUNDS **5a-e** AND **7a-f**

Molecules	hERG	H-HT	Ames	HIA	PPB	BBB	Pgp_inh	CYP1A2-I	CYP2C19-I	CYP2C9-I	CYP2D6-I	CYP3A4-I
5a	0.427	0.880	0.967	0.0001	95.2	0.034	0.274	0.004	0.999	0.999	0.003	0.999
5b	0.426	0.783	0.825	0.002	96.0	0.269	0.381	$6.8xe^{-05}$	0.999	0.999	0.0004	0.999
5c	0.391	0.761	0.751	0.0001	96.6	0.494	0.702	0.001	0.999	0.999	0.0002	0.999
5d	0.360	0.756	0.761	$5.8.e^{-05}$	95.7	0.798	0.329	0.007	0.999	0.999	0.0034	0.999
5e	0.284	0.731	0.804	$8.1.e^{-05}$	92.2	0.851	0.006	0.001	0.999	0.995	$5.3.e^{-05}$	0.999
7a	0.221	0.708	0.562	0.0002	96.5	0.775	0.424	0.020	0.999	0.999	0.054	0.999
7b	0.606	0.522	0.715	0.017	87.0	0.087	0.215	$6.3xe^{-05}$	0.996	0.998	0.899	0.999
7c	0.433	0.691	0.946	0.0004	94.46	0.023	0.128	0.0001	0.975	0.999	0.182	0.913
7d	0.360	0.756	0.761	$5.8.e^{-05}$	95.72	0.798	0.329	0.0072	0.999	0.999	0.003	0.999
7e	0.503	0.527	0.741	0.017	96.36	0.084	0.285	0.0006	0.954	0.999	0.314	0.997
7f	0.465	0.592	0.643	0.0009	95.98	0.471	0.631	0.0007	0.910	0.999	0.480	0.944
LVF	0.255	0.989	0.734	$2.6.e^{-06}$	23.43	0.556	$6.3xe^{-06}$	$1.8xe^{-08}$	$8.3xe^{-06}$	$6.2xe^{-06}$	$2.4xe^{-06}$	$7.7xe^{-09}$

For the classification endpoints, the prediction probability values are transformed into six symbols: 0-0.1 (---), 0.1-0.3 (--), 0.3-0.5 (-), 0.5-0.7 (+), 0.7-0.9 (++) and 0.9-1.0 (+++).

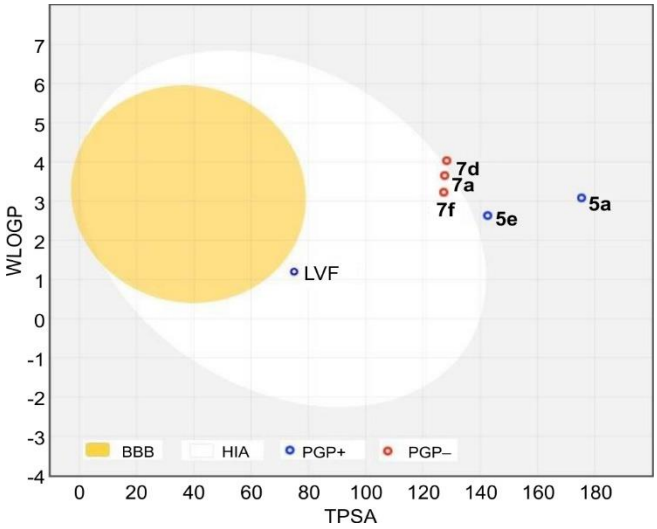

Fig. 6. SwissADME boiled-egg plot for most active triazole scaffolds

Conclusion

A novel series of 1,3,4-oxadiazole derivatives incorporating acetamide and 1,2,3-triazole moieties was designed and synthesized as potential inhibitors of bacterial DNA gyrase and topoisomerase IV. All compounds were characterized using ^{1}H NMR, ^{13}C NMR, FTIR and HRMS. Structure–activity relationships (SARs) were evaluated by based on synthetic pathways, antimicrobial activities and molecular docking studies. The results revealed that all synthesized compounds exhibited significant antibacterial and antifungal activities. Further based on the investigation, compounds **5a**, **5e**, **7a** and **7d** demonstrated significant antibacterial and antifungal activities, surpassing standard drugs levofloxacin (LVF) and clotrimazole (CLZ). Given their superior antibacterial profiles, molecular docking studies were subsequently performed for compounds **5a**, **7a** and **7d**. This investigation revealed multiple interactions between the ligands and the active sites of DNA gyrase and topoisomerase IV, including hydrogen bonds, C–H bonds, hydrophobic contacts and van der Waals forces. Moreover, SwissADME, was employed to evaluate the drug-likeness, pharmacokinetic properties and physicochemical characteristics of the synthesized compounds. The results indicated that these compounds possess favourable ADME profiles. Overall, the findings of this study are highly promising for the development of new antimicrobial agents, particularly given the clinical significance of the tested microorganisms.

ACKNOWLEDGEMENTS

One of the authors (PP) is thankful to United States Pharmacopeia India (P) Ltd., Hyderabad, and Department of Chemistry, Koneru Lakshmaiah Education Foundation (KLEF), Guntur for providing the required facilities and motivation for the completion of the research work. Sincere thanks are also extended to Osmania University for their support in carrying out the molecular docking studies and biological evaluations.

CONFLICT OF INTEREST

The authors declare that there is no conflict of interests regarding the publication of this article.

REFERENCES

1. S.S. AlNeyadi, A.A. Salem, M.A. Ghattas, N. Atatreh and I.M. Abdou, *Eur. J. Med. Chem.*, **136**, 270 (2017); https://doi.org/10.1016/j.ejmech.2017.05.010
2. L. Suresh, P. Sagar Vijay Kumar, Y. Poornachandra, C. Ganesh Kumar and G.V.P. Chandramouli, *Bioorg. Med. Chem. Lett.*, **27**, 1451 (2017); https://doi.org/10.1016/j.bmcl.2017.01.087
3. P.K. Sharma, N. Chandak, P. Kumar, C. Sharma and K.R. Aneja, *Eur. J. Med. Chem.*, **46**, 1425 (2011); https://doi.org/10.1016/j.ejmech.2011.01.060
4. D. Kruszewska, H.-G. Sahl, G. Bierbaum, U. Pag, S.O. Hynes and Å. Ljungh, *J. Antimicrob. Chemother.*, **54**, 648 (2004); https://doi.org/10.1093/jac/dkh387
5. A.K. Dunga, T.R. Allaka, Y. Kethavarapu, S.K. Nechipadappu, P. Pothana, K. Ravada, J. Kashanna and P.V.V.N. Kishore, *Results Chem.*, **4**, 100605 (2022); https://doi.org/10.1016/j.rechem.2022.100605
6. I.M. Gould and A.M. Bal, *Virulence*, **4**, 185 (2013); https://doi.org/10.4161/viru.22507
7. M.A. Salam, M.Y. Al-Amin, M.T. Salam, J.S. Pawar, N. Akhter, A.A. Rabaan and M.A.A. Alqumber, *Healthcare*, **11**, 1946 (2023); https://doi.org/10.3390/healthcare11131946
8. V. Straniero, *Antibiotics*, **13**, 171 (2024); https://doi.org/10.3390/antibiotics13020171
9. N. Kerru, L. Gummidi, S. Maddila, K.K. Gangu and S.B. Jonnalagadda, *Molecules*, **25**, 1909 (2020); https://doi.org/10.3390/molecules25081909
10. M.M. Heravi and V. Fathi-Vavsari, in eds.: E.F.V. Scriven and C.A. Ramsden, Recent Advances in Application of Amino Acids: Key Building Blocks in Design and Syntheses of Heterocyclic Compounds; In: Advances in Heterocyclic Chemistry, Academic Press, Chap. 2, vol. 114, pp 77 (2015).
11. K. Bozorov, J. Zhao and H.A. Aisa, *Bioorg. Med. Chem.*, **27**, 3511 (2019); https://doi.org/10.1016/j.bmc.2019.07.005
12. N. Nehra, R.K. Tittal and V.D. Ghule, *ACS Omega*, **6**, 27089 (2021); https://doi.org/10.1021/acsomega.1c03668
13. V.S.R. Avuthu, T.R. Allaka, P.R. Patel, S. Venkatesan, N. Honnappa, M. Afzal and P.V.V.N. Kishore, *J. Mol. Struct.*, **1314**, 138736 (2024); https://doi.org/10.1016/j.molstruc.2024.138736
14. A. Basireddy, T.R. Allaka, A.R. Allam, S.R. Baddam, S. Basireddy and P.V.V.N. Kishore, *Curr. Org. Chem.*, **27**, 1882 (2023); https://doi.org/10.2174/0113852728276712231123111714
15. Ş.G. Küçükgüzel, E.E. Oruç, S. Rollas, F. Şahin and A. Özbek, *Eur. J. Med. Chem.*, **37**, 197 (2002); https://doi.org/10.1016/S0223-5234(01)01326-5
16. G. Venkateswara Rao, T.R. Allaka, M.K. Gandla, P.K. Veera Venkata Nanda, S.R. Pindi, P.R.R. Vaddi and H.B. Bollikolla, *J. Heterocycl. Chem.*, **60**, 1666 (2023); https://doi.org/10.1002/jhet.4700
17. S.V. Bhandari, K.G. Bothara, M.K. Raut, A.A. Patil, A.P. Sarkate and V.J. Mokale, *Bioorg. Med. Chem.*, **16**, 1822 (2008); https://doi.org/10.1016/j.bmc.2007.11.014
18. B. Alburquerque-González, Á. Bernabé-García, M. Bernabé-García, J. Ruiz-Sanz, F.F. López-Calderón, L. Gonnelli, L. Banci, J. Peña-García, I. Luque, F.J. Nicolás, M.L. Cayuela-Fuentes, E. Luchinat, H. Pérez-Sánchez, S. Montoro-García and P. Conesa-Zamora, *Cancers*, **13**, 861 (2021); https://doi.org/10.3390/cancers13040861
19. P. Mishra, G.K. Joshi, A.K. Shakya, R.K. Agrawal and G.K. Patnaik, *Indian J. Pharmacol.*, **36**, 247 (1992).
20. X.-M. Zhang, M. Qiu, J. Sun, Y.-B. Zhang, Y.-S. Yang, X.-L. Wang, J.-F. Tang and H.-L. Zhu, *Bioorg. Med. Chem.*, **19**, 6518 (2011); https://doi.org/10.1016/j.bmc.2011.08.013
21. A. Zarghi, S.A. Tabatabai, M. Faizi, A. Ahadian, V. Zanganeh, P. Navabi, and A. Shafiee, *Bioorg. Med. Chem. Lett.*, **15**, 1863 (2005); https://doi.org/10.1016/j.bmcl.2005.02.014
22. J.H. Musser, R.E. Brown, B. Loev, K. Bailey, H. Jones, R. Kahen, F. Huang, A. Khandwala and M. Leibowitz, *J. Med. Chem.*, **27**, 121 (1984); https://doi.org/10.1021/jm00368a004
23. Y. Wang, H. Zhang, W. Shen, P. He and Z. Zhou, *J. Cancer Res. Clin. Oncol.*, **144**, 1751 (2018); https://doi.org/10.1007/s00432-018-2664-y

24. O. Sheikh and T. Yokota, *Expert Opin. Investig. Drugs*, **30**, 167 (2021); https://doi.org/10.1080/13543784.2021.1868434
25. W. Berger, F. Hampel Jr., J. Bernstein, S. Shah, H. Sacks and E.O. Meltzer, *Ann. Allergy Asthma Immunol.*, **97**, 375 (2006); https://doi.org/10.1016/S1081-1206(10)60804-6
26. E.N. Scott, G. Meinhardt, C. Jacques, D. Laurent and A.L. Thomas, *Expert Opin. Investig. Drugs*, **16**, 367 (2007); https://doi.org/10.1517/13543784.16.3.367
27. S. Hasabelnaby, E.M. Mohi El-Deen and A. Goudah, *Antiinflamm. Antiallergy Agents Med. Chem.*, **14**, 148 (2015); https://doi.org/10.2174/1871523014666151103113544
28. A.D. Lebsack, J. Gunzner, B. Wang, R. Pracitto, H. Schaffhauser, A. Santini, J. Aiyar, R. Bezverkov, B. Munoz, W. Liu and S. Venkatraman, *Bioorg. Med. Chem. Lett.*, **14**, 2463 (2004); https://doi.org/10.1016/j.bmcl.2004.03.008
29. Q.-R. Zhang, D.-Q. Xue, P. He, K.-P. Shao, P.-J. Chen, Y.-F. Gu, J.-L. Ren, L.-H. Shan and H.-M. Liu, *Bioorg. Med. Chem. Lett.*, **24**, 1236 (2014); https://doi.org/10.1016/j.bmcl.2013.12.010
30. Y.E. Sherif, R. Alansari and M.A. Gouda, *Antiinflamm. Antiallergy Agents Med. Chem.*, **17**, 3 (2018); https://doi.org/10.2174/1871523017666180413111321
31. Y.E. Sherif, M.A. Gouda and A.A. El-Asmy, *Med. Chem. Res.*, **24**, 3853 (2015); https://doi.org/10.1007/s00044-015-1427-4
32. M.S. Behalo, I.A. Gad El-karim and R. Rafaat, *J. Heterocycl. Chem.*, **54**, 3591 (2017); https://doi.org/10.1002/jhet.2985
33. W.M. Eldehna, H. Almahli, G.H. Al-Ansary, H.A. Ghabbour, M.H. Aly, O.E. Ismael, A. Al-Dhfyan and H.A. Abdel-Aziz, *J. Enzyme Inhib. Med. Chem.*, **32**, 600 (2017); https://doi.org/10.1080/14756366.2017.1279155
34. G. Gogisetti, U. Kanna, V. Sharma, T. Rao Allaka and B.R. Tadiboina, *Chem. Biodivers.*, **19**, e202200681 (2022); https://doi.org/10.1002/cbdv.202200681
35. J.C. McPherson III, R. Runner, T.B. Buxton, J.F. Hartmann, D. Farcasiu, I. Bereczki, E. Rőth, S. Tollas, E. Ostorházi, F. Rozgonyi and P. Herczegh, *Eur. J. Med. Chem.*, **47**, 615 (2012); https://doi.org/10.1016/j.ejmech.2011.10.049
36. M. Hu, J. Li and S.Q. Yao, *Org. Lett.*, **10**, 5529 (2008); https://doi.org/10.1021/ol802286g
37. G.L. French, *J. Antimicrob. Chemother.*, **58**, 1107 (2006); https://doi.org/10.1093/jac/dkl393
38. I. Castillo-Juárez, F. Rivero-Cruz, H. Celis and I. Romero, *J. Ethnopharmacol.*, **114**, 72 (2007); https://doi.org/10.1016/j.jep.2007.07.022
39. E.J.L. Stéen, D.J. Vugts and A.D. Windhorst, *Front. Nucl. Med.*, **2**, 853475 (2022); https://doi.org/10.3389/fnume.2022.853475
40. G. Venkanna, A.T. Rao, K.S. Kumar, M.S.N.A. Prasad, C. Kalyani, G.S. Kumar and V. Srinivas, *Russ. J. Bioorg. Chem.*, **50**, 1519 (2024); https://doi.org/10.1134/S1068162024040277
41. A. Daina, O. Michielin and V. Zoete, *Sci. Rep.*, **7**, 42717 (2017); https://doi.org/10.1038/srep42717
42. S.K. Konda, S. Kuna, S. Pandiri, P. Akarapu, S. Bhoomandla and P.V.V.N. Kishore, *Bull. Chem. Soc. Ethiop.*, **39**, 731 (2025); https://doi.org/10.4314/bcse.v39i4.10
43. V. Gujja, K. Sadineni, M.R. Epuru, T. Rao Allaka, V. Banothu, S.K. Gunda and S.K. Koppula, *Chem. Biodivers.*, **20**, e202301232 (2023); https://doi.org/10.1002/cbdv.202301232
44. S. Bellon, J.D. Parsons, Y. Wei, K. Hayakawa, L.L. Swenson, P.S. Charifson, J.A. Lippke, R. Aldape and C.H. Gross, *Antimicrob. Agents Chemother.*, **48**, 1856 (2004); https://doi.org/10.1128/AAC.48.5.1856-1864.2004
45. B.D. Bax, P.F. Chan, D.S. Eggleston, A. Fosberry, D.R. Gentry, F. Gorrec, I. Giordano, M.M. Hann, A. Hennessy, M. Hibbs, J. Huang, E. Jones, J. Jones, K.K. Brown, C.J. Lewis, E.W. May, M.R. Saunders, O. Singh, C.E. Spitzfaden, C. Shen, A. Shillings, A.J. Theobald, A. Wohlkonig, N.D. Pearson and M.N. Gwynn, *Nature*, **466**, 935 (2010); https://doi.org/10.1038/nature09197
46. S.K. Gandham, A.A. Kudale, T.R. Allaka, K. Chepuri and A. Jha, *J. Mol. Struct.*, **1295**, 136714 (2024); https://doi.org/10.1016/j.molstruc.2023.136714
47. R.A. Laskowski, J. Jabłońska, L. Pravda, R.S. Vařeková and J.M. Thornton, *Protein Sci.*, **27**, 129 (2018); https://doi.org/10.1002/pro.3289
48. K. Sadineni, S. Reddy Basireddy, T. Rao Allaka, S. Bhoomandla, S. Yatam, V. Muvvala and S. Babu Haridasyam, *Chem. Biodivers.*, **21**, e202400389 (2024); https://doi.org/10.1002/cbdv.202400389
49. S. Dallakyan and A.J. Olson, *Methods Mol. Biol.*, **1263**, 243 (2015); https://doi.org/10.1007/978-1-4939-2269-7_19